

Application Of Regular Falsi Algorithm In The Determination Of The Optimal Path Length For Terrestrial Fixed Point Microwave Line Of Sight Communication Link

Isaac A. Ezenugu¹

Department of Electrical/Electronic Engineering, Imo State University, Owerri, Nigeria
isaac.ezenugu@yahoo.com

Ezeh, Ikechukwu H.²

Department of Electrical/Electronic Engineering, Imo State University, Owerri, Nigeria

Abstract— In this paper, application of Regular Falsi algorithm in the determination of the optimal path length for terrestrial fixed point microwave line of sight communication link is presented. Relevant mathematical expressions for the computation of path length of microwave line of sight (LOS) link are presented along with the theory of Regular Falsi algorithm. Further, Regular Falsi algorithm was adapted to the optimal path length computation and based on the optimal conditions specified in the mathematical analysis. The performance of the algorithm is expressed in terms of convergence cycle which is the minimum number of iteration of the algorithm at which the optimal path length value is attained. Some sample numerical examples were conducted. Particularly, at Ku frequency of 10GHz, for the sample site examined Regular Falsi. The performance of the algorithm was expressed as the convergence cycle, which is the minimum number of iteration at which the optimal path length is obtained. The effect of frequency on the performance of the algorithm was also performed. In all, the Regular Falsi algorithm maintained the same convergence cycle in all the microwave frequencies considered.

Keywords— Microwave Link, Path Length, Regular Falsi Algorithm, Convergence Circle, Optimal Path Length, Numerical iteration methods, Line of sight communication

I. INTRODUCTION

Over the years line of sight (LOS) terrestrial microwave communication is used to provide communication over a large area by using multiple hops of transmitter and receiver stations antennas arranged in a LOS fashion to ensure good reception of the signal [1,2]. The distance between the transmitter and receiver is referred to as the path length [3,4,5,6,7]. In order to reduce cost, most often the maximum path length is used in the design. This path length is computed based on the knowledge of the path loss and the fade margin specified at the design time. Particularly, the fade margin is meant to account for expected fade depth due to rain or multipath fade mechanisms [8,9,10].

However, designers rely on the maximum path length obtained from the path loss without verifying if the fade depth the will occur over the maximum path length can be accommodated by the specified fade margin. In such case, the system will have more outages than what is specified by the design should the fade depth be greater than the specified fade margin.

Available study on this issue opted for optimal path length which is the path length at which the available fade margin is just enough to accommodate the maximum fade depth the signal will encounter along the path [12].

In microwave design, determination of the optimal path length requires iteration process to repeatedly select the path length and evaluate it for optimality until the optimal value is attained. Previous study used the Newton Raphson method [12]. Although Newton Raphson method converges fast, however, it requires some extra mathematical processes that make it difficult to apply in some cases [13,14,15]. Also, Bisection method can be simpler to implement but its convergence performance is quite slow [15,16,17,18]. As such in this paper, the Regular Falsi algorithm is employed in the determination of the optimal path length [19] of a point-to-point LOS microwave communication link. The Regular Falsi method is an improved version of the Bisection method which converges faster than the classical Bisection method and at the same time it is easier to implement when compare with the Newton Raphson method [20,21,22,23,24]. The relevant mathematical expressions that facilitate the computation of the optimal path length are presented along with explanation and flowchart on how the Regular Falsi method can be used to determine the optimal path length. Sample numerical examples are presented as well as the performance analysis of the algorithm in terms of its convergence cycle and the sensitivity of the convergence cycle to frequency.

II .THE MATHEMATICAL EXPRESSIONS FOR COMPUTING OPTIMAL PATH LENGTH OF TERRESTRIAL POINT-TO-POINT MICROWAVE LINK

The Free Space Path Loss (LFSP) is given as [25,26,27,28];

$$LFSP = 32.4 + 20 \log(f*1000) + 20 \log(d) \quad (1)$$

where frequency in GHz is denoted as f and the path length in km is denoted as d .

The received signal (PR) for terrestrial point to point microwave link is given as [29,30,31,32]:

$$P_R = f m_s + P_s = P_T + (G_T + G_R) - LFSP \quad (2)$$

Where P_R is the Received Signal Power (dBm); $f m_s$ is the fade margin (dB); P_s is the receiver sensitivity (dB); P_T is transmitter power output (dBm); G_T is transmitter antenna gain (dBi); G_R is receiver antenna gain (dBi) and LFSP is free space path loss (dB).

The maximum transmission range based on Free Space Path Loss (LFSP) is given from Equations 1 and as

$$d = 10^{\left(\frac{(P_T + G_T + G_R - f m_s - P_s) - 32.4 - 20 \log(f*1000)}{20}\right)} \quad (3)$$

The rain fade depth (A_{Rain}) in dB can be determined using ITU-R PN.838 recommendations as follows [33,34]:

$$A_{Rain} = \text{maximum} \left((k_v (R_{po})^{\alpha_v}), k_h (R_{po})^{\alpha_h} \right) d \quad (4)$$

Where $\gamma_{R_{po}}$ in dB/km is the specific attenuation originating from rainfall; R_{po} is the rainfall rate in mm/h exceeded for $Po\%$ of an average year, d is the path length and k_v , α_v , k_h and α_h are frequency dependent for vertical and horizontal polarizations. The multipath fade depth, $A_{multipath}$ (in dB) is obtain from ITU quick planning applications model for Po as follows [35, 36, 37, 38];

$$A_{multipath} = 10(-0.00089h_L) - (10) \log \left(\frac{po}{\left\{ \frac{K(d^{3.1})(1+|\epsilon_p|)^{-1.29}}{(0.8)} \right\}} \right) \quad (5)$$

Where frequency in GHz is denoted as f ; path length in km is denoted as d ; the altitude of the lower antenna in meters is denoted as h_L ; the point refractivity gradient is denoted as $dN1$; the path inclination is ϵ_P and the geoclimatic factor is denoted as K where:

$$K = 10^{(-4.6 - 0.0027dN1)} \quad (7)$$

The path inclination, ϵ_P is calculated as follows;

$$|\epsilon_P| = \frac{(h_t - h_r)}{d} \quad (8)$$

where:

d is the propagation path length in km; h_t is the antenna transmitter antenna height and h_r is the receiver transmitter antenna height (where h_t and h_r are in meters about sea level), :

$$h_L = \text{minimum}(h_t, h_r) \quad (9)$$

The link effective fade depth ($f d_m$) is computed as follows;

$$f d_m = \text{maximum}(A_{multipath}, A_{Rain}) \quad (12)$$

The optimal path length (d_{mop}) is obtain when the following condition is fulfilled;

$$f d_m - P_R - P_S = 0 \quad (13)$$

For high-frequency microwave signal rain fading mechanism dominates hence, $f d_m = A_{Rain}$;

$$A_{Rain} - (P_R - P_S) = 0 \quad (14)$$

III. APPLICATION OF REGULAR FALSI ALGORITHM FOR DETERMINATION OF THE OPTIMAL PATH LENGTH OF TERRESTRIAL MICROWAVE LINK

In Regular Falsi algorithm, for a given function, $f(x)$ the root is found by first selecting or guessing two initial root values a and b where $a < b$ to give an initial interval a to b such that, $f(a)*f(b) < 0$. The expected root, x of the function, $f(x)$ is computed as follows;

$$x = \frac{a*f(b) - b*f(a)}{f(b) - f(a)} \quad (15)$$

If $f(x) = 0$ the root is x otherwise two other roots are obtained from the values of a , b and x according to the Regular Falsi flowchart of Figure 1.

In order to apply the Regular Falsi algorithm to the optimal path length, the value of a and b are determined as follows;

$b = d$ (where d is the path length given in given in Equation 3)

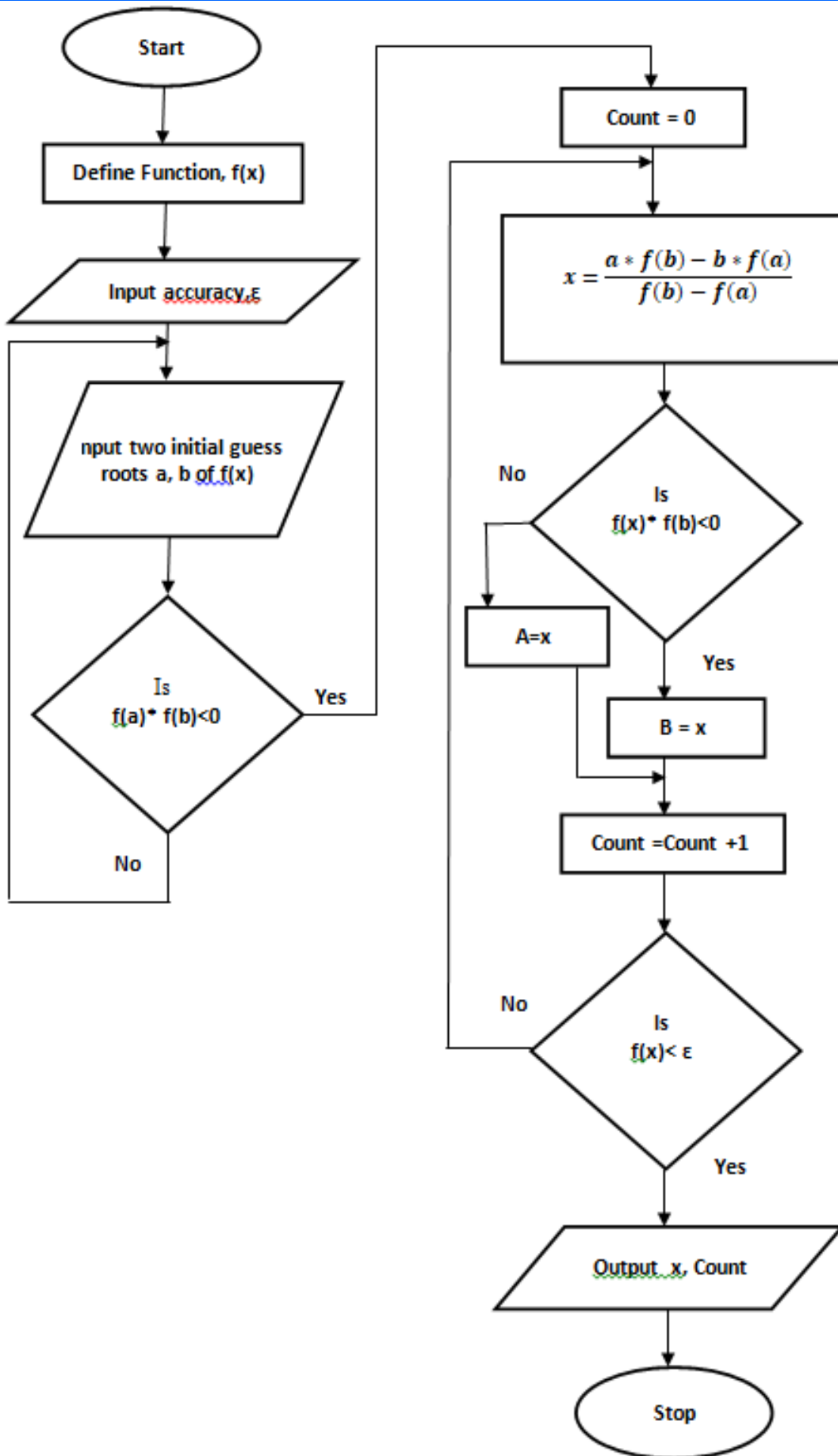


Figure 1 Flowchart For Regular Falsi Method

In order to obtain the second initial root , another path length d_{rain} is determined. In Equation 4 the rain attenuation, A_{Rain} was computed using the maximum path length obtained from free space path loss, FSPL and the available fade margin, $P_R - P_S$ as shown in Equation 3. However, d_{rain} which is the path length due to specific rain fading and the available fade margin is given from Equation 4 and Equation 14 as follows ;

$$\text{Maximum} \left((k_v(R_{po})^{\alpha_v}), k_h(R_{po})^{\alpha_h} \right) d_{rain} = P_R - P_S \quad (16)$$

$$d_{rain} = \frac{P_R - P_S}{\text{maximum} \left((k_v(R_{po})^{\alpha_v}), k_h(R_{po})^{\alpha_h} \right) d_{rain}} \quad (17)$$

So, in Figure 1, the function $f(x)$ is actually $f(d)$ where $b = d$, $a = d_{rain}$ and the function is given in Equation 13 or Equation 14 as

$$f(x) = f(d) = f d_m - P_R - P_S \quad (18)$$

$$f(x) = f(d) = A_{Rain} - P_R - P_S \quad (19)$$

In the flowchart of Figure 1, the iteration counter value printed at the end of the iteration gives the minimum number of iterations at which the algorithm converged with a given optimal path length. The

IV. RESULTS AND DISCUSSION

In the numerical example a 10 GHz microwave line of sight communication link is considered the link parameters as shown in Table 1.

Table 1 The microwave line of sight communication link and site parameters

S/N	Parameter Name	Parameter Value and Unit
1	Frequency	10 GHz
2	Transmitter Power	13 dB
3	Transmitter Antenna Gain	32 dBi
4	Receiver Antenna Gain	32 dBi
5	Receiver Sensitivity	-78 dB
6	Fade Margin	18 dB
7	Network Percentage Availability	99.99 %,
8	ITU rain zone of the case study site	N
9	Rain Rate Of The Case Study Site	95 mm/hr
10	Rain Fading Constants Are k_H	0.01217
11	Rain Fading Constants Are a_H	1.2571
12	Rain Fading Constants Are k_v	0.01129
13	Rain Fading Constants Are a_v	1.2156
14	Point Refractivity Gradient (dN1)	-400
15	Initial Free Space Path loss	137.04 dB

The result of the iterations in computing the optimal path length using the Regular Falsi method is shown in Table 2, Table 3 , Figure 2 and Figure 4. According to the result in Table 2 and data in Table 1, with the initial free space path loss of 137.04 dB along with the specified fade margin of 18 dB and receiver sensitivity of -78 dB the maximum path length of the link is determined as 16.9824 Km. At the 5th iteration or cycle the algorithm converged with effective optimal path length of 7.5127 Km which is about 55.76 % reduction in path length from the initial value of 16.9824 Km. At this optimal path length of 7.5127 Km, the effective fade margin is 25.0841 dB which is the same as the fade depth at the optimal path length. This means that the link can accommodate the maximum fade depth of 25.0841 dB which the signal can experience in the link without going into network outage. This is not the case at the initial point where the fade margin specified is 18 dB whereas the fade depth is 56.7025 dB. Furthermore, Table 3 and Figure 3 show that the received signal strength will increase from -60 dB at the initial value to -54.13 dB at the optimal path length.

performance of the algorithm is indicated by the convergence cycle; the smaller the convergence cycle the faster and better the performance of the algorithm.

Since the path length , the free space path loss , rain fade depth and other link parameters are functions of frequency , the algorithm will be used on microwave link operating at different frequencies. Then, sensitivity analysis will be carried out on the output of the algorithm to quantify how frequency affect the performance of the algorithm. The sensitivity analysis is conducted as follows; given two variable X_i and Y_i where $i = 0, 1, 2, \dots, n$, then the sensitivity , S_i of Y_i with respect to X_i is given as ;

$$S_i = \left(\frac{X_{(i+1)} - X_i}{X_i} \right) \left(\frac{Y_{(i+1)} - Y_i}{Y_i} \right) \quad (20)$$

The sensitivity gives the number of units of change in Y for every unit change in X. For instance, if X is frequency in GHz and Y is path length in Km, then the sensitivity of path length with respect to frequency is interpreted as the number of Km change in path length that will occur for any 1 GHz change if frequency. It is the same thing as the percentage change in X divided by the percentage change in Y.

Table 2: Free Space Path Loss , Effective Fade Margin, Effective Fade Depth, and Effective Path Length vs Number of Iterations (n)

Number Of Iterations (n)	Free Space Path Loss	Effective Fade Margin	Effective Fade Depth	Differential Path Length	Effective Path Length
0	137.0400	17.9600	56.7025	-11.6034	16.9824
1	127.0541	27.9859	17.9600	3.0028	5.3790
2	130.2444	24.7956	25.9313	-0.3402	7.7664
3	129.9684	25.0716	25.1202	-0.0146	7.5235
4	129.9565	25.0835	25.0856	-0.0006	7.5132
5	129.9559	25.0841	25.0841	0.0000	7.5127
6	129.9559	25.0841	25.0841	0.0000	7.5127
7	129.9559	25.0841	25.0841	0.0000	7.5127
8	129.9559	25.0841	25.0841	0.0000	7.5127
9	129.9559	25.0841	25.0841	0.0000	7.5127
10	129.9559	25.0841	25.0841	0.0000	7.5127

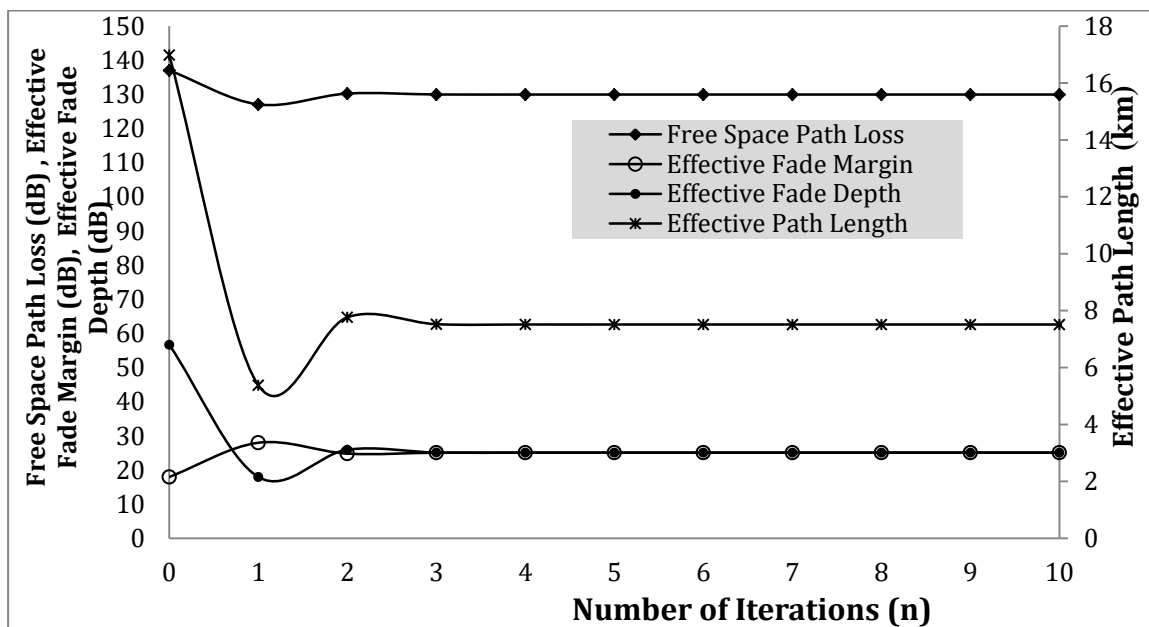


Figure 2: Free Space Path Loss , Effective Fade Margin, Effective Fade Depth, and Effective Path Length vs Number of Iterations (n)

Table 3: The Initial and the optimal values of key link parameters and the convergence cycle

	n	Path Length (km)	Free Space Path Loss (dB)	Fade Margin (dB)	Fade Depth (dB)	Received Power (dBm)
Initial parameter value	0	16.98	137.04	18.00	56.70	-60.00
Optimal parameter Value	5	8.64	131.17	23.87	28.83	-54.13

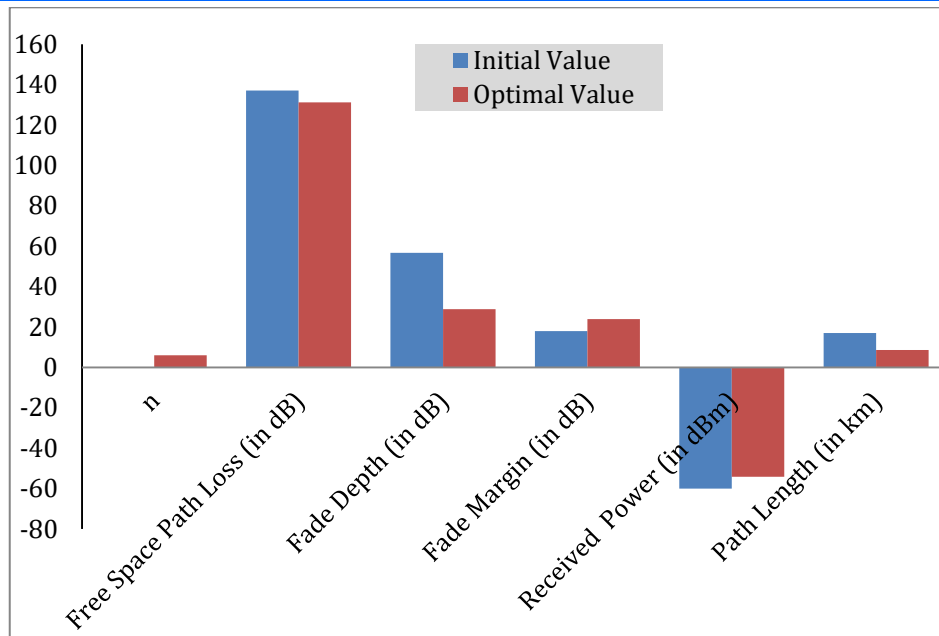


Figure 3: The Initial and the optimal values of key link parameters and the convergence cycle

Table 4: Differential Fade Depth and Effective Path Length vs Number of Iterations (i)

Number Of Iterations (n)	Differential Fade Depth	Effective Path Length (de)
0	38.7425	16.9824
1	-10.0259	5.3790
2	1.1357	7.7664
3	0.0486	7.5235
4	0.0021	7.5132
5	0.0000	7.5127
6	0.0000	7.5127
7	0.0000	7.5127
8	0.0000	7.5127
9	0.0000	7.5127
10	0.0000	7.5127

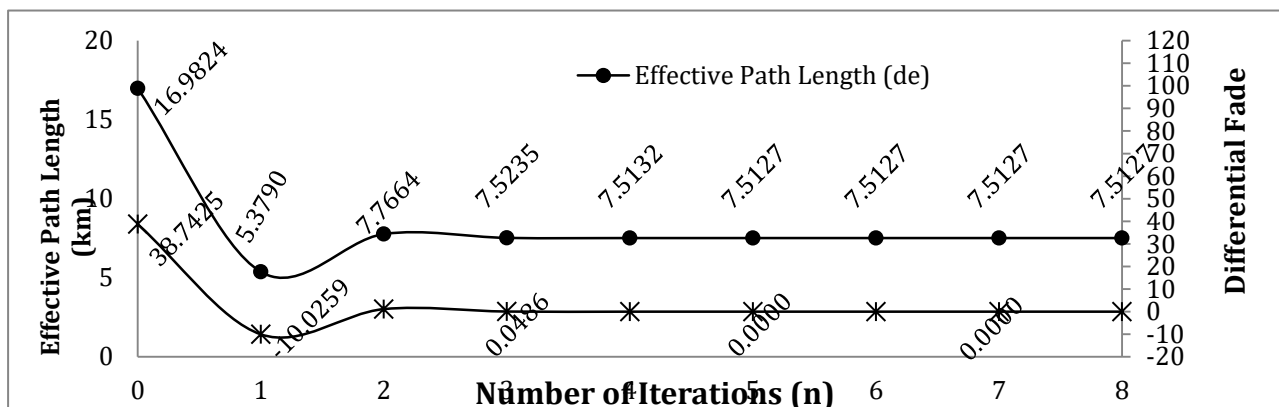


Figure 4: Differential Fade Depth and Effective Path Length vs Number of Iterations (n)

The way the differential fade depth and effective path length vary with the number of iterations (i) is shown in Table 4 and Figure 4. The differential fade depth is the between the value of the fade depth at iteration i and i+1.

The algorithm converges when the differential fade depth is zero. As the differential fade depth tends to zero, the effective path length tends to the optimal path length.

The results on the effect of frequency on the convergence cycle of the Regular Falsi algorithm for optimal path length are shown in Table 5 and Figure 5 as well as in Table 6 and Figure 6. The convergence cycle remains constant at 5 for all the frequencies considered. On the other hand, both optimal path length and initial path length decreased with frequency.

The results on the sensitivity of the Convergence Cycle, Optimal Path Length, Optimal Fade Depth and Optimal Path Loss with frequency are given in Table 7 and Figure 7. Again, the convergence cycle does not vary with frequency, hence it has a sensitivity of zero. As regards optimal path length, the results show that every 1 GHz increase in frequency causes a decrease in the optimal path length. However, the amount by which the optimal path length decreases reduces as frequency increases. In all, optimal path length, optimal fade depth and optimal path loss are sensitive to frequency whereas the convergence cycle is not.

Table 5: The Convergence Cycle, the Optimal Path Length, the Initial Path Length and vs frequency

f (GHz)	Optimal Path Length (km)	Initial Path Length (km)	Convergence Cycle
12	5.15	14.15	5
15	3.71	11.32	5
18	2.90	9.43	5
21	2.38	8.09	5
24	2.03	7.08	5
27	1.79	6.29	5
30	1.60	5.66	5
33	1.46	5.15	5
36	1.36	4.72	5
39	1.27	4.35	5
42	1.20	4.04	5
45	1.14	3.77	5

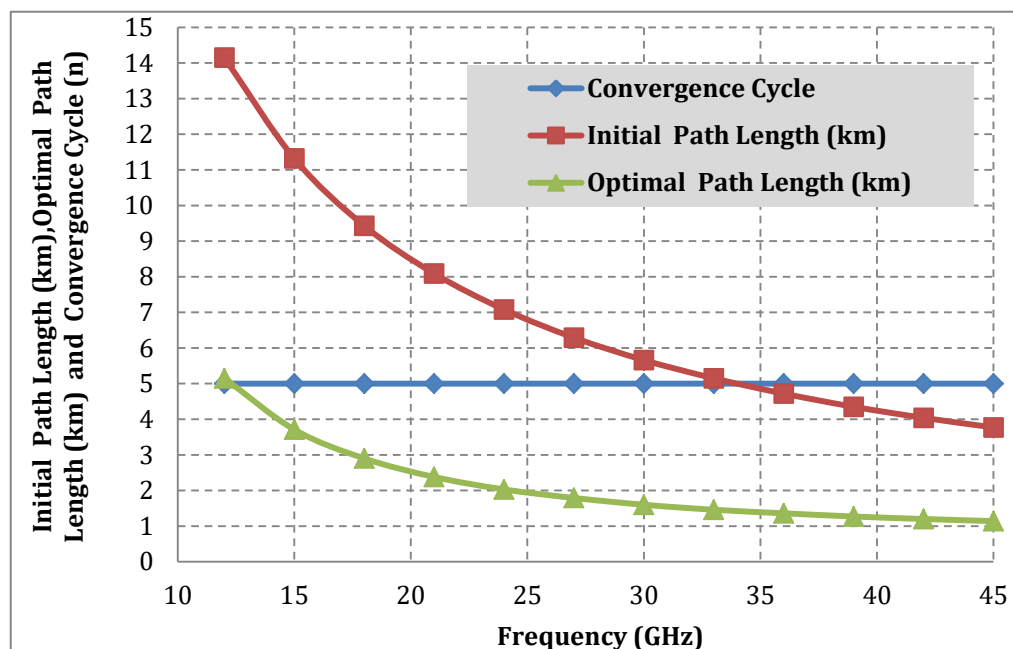


Figure 5: The Convergence Cycle, the Optimal Path Length, the Initial Path Length and vs frequency

Table 6: Optimal Path Length, Optimal Fade Depth, Optimal Path Loss and Convergence Cycle vs frequency

f (GHz)	Convergence Cycle	Optimal Path Length (Km)	Optimal Fade Depth (dB)	Optimal Path loss (dB)
12	5	5.1	26.8	128.3
15	5	3.7	27.7	127.3
18	5	2.9	28.3	126.8
21	5	2.4	28.6	126.4
24	5	2.0	28.8	126.2
27	5	1.8	28.9	126.1
30	5	1.6	29.0	126.1
33	5	1.5	28.9	126.1
36	5	1.4	28.8	126.2
39	5	1.3	28.7	126.3
42	5	1.2	28.5	126.5
45	5	1.1	28.4	126.7

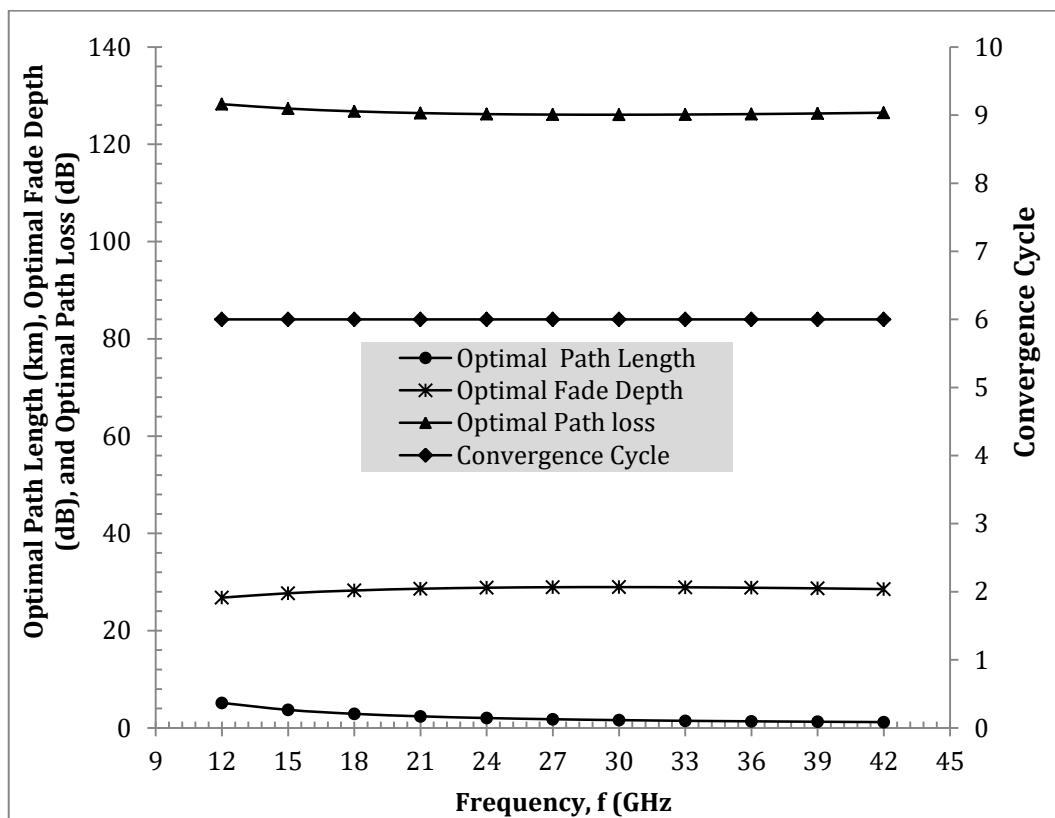


Figure 6: Optimal Path Length, Optimal Fade Depth , Optimal Path Loss and Convergence Cycle vs frequency

Table 7: Sensitivity of Convergence Cycle, Optimal Path Length , Optimal Fade Depth and Optimal Path loss on Frequency

f (GHz)	Sensitivity of Convergence Cycle With frequency	Sensitivity of Optimal Path Length With frequency	Sensitivity of Optimal Fade Depth With frequency	Sensitivity of Optimal Path Loss With frequency
12	0.00	-1.12	0.14	-0.03
15	0.00	-1.10	0.10	-0.02
18	0.00	-1.07	0.08	-0.02
21	0.00	-1.02	0.05	-0.01
24	0.00	-0.97	0.03	-0.01
27	0.00	-0.92	0.01	0.00
30	0.00	-0.87	-0.01	0.00
33	0.00	-0.81	-0.03	0.01
36	0.00	-0.76	-0.05	0.01
39	0.00	-0.71	-0.07	0.02
42	0.00	-0.67	-0.09	0.02

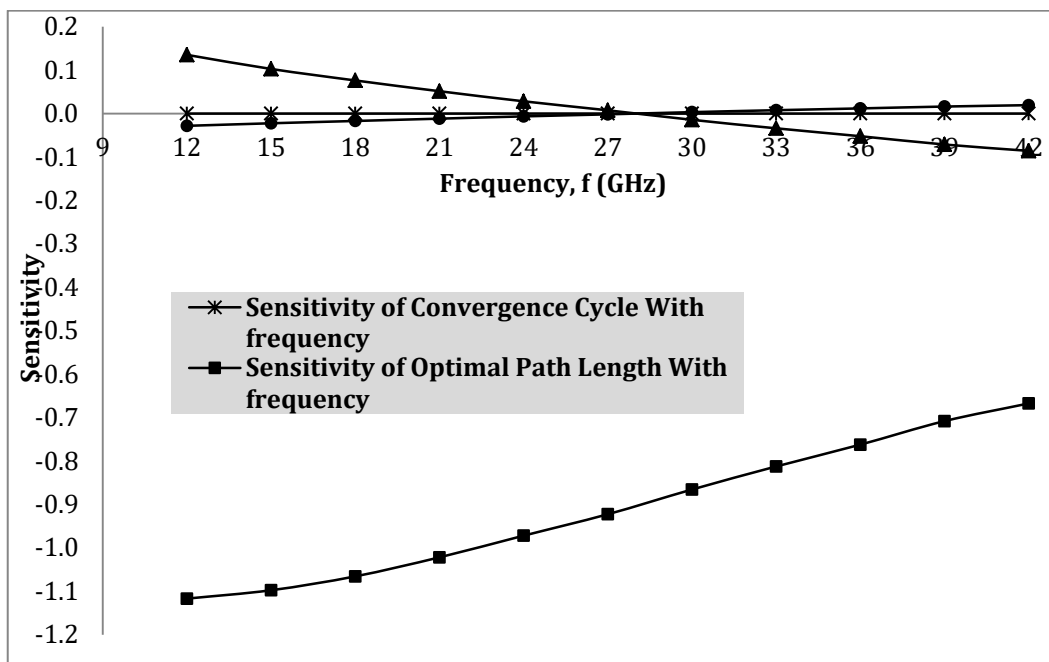


Figure 7: Sensitivity of Convergence Cycle, Optimal Path Length , Optimal Fade Depth and Path loss on Frequency

V. CONCLUSION

Regular Falsi numerical iteration algorithm is adapted and used to determine the optimal path length of a microwave communication link. Some sample numerical examples were conducted. The performance of the algorithm was expressed as the in all the microwave frequencies considered.

convergence cycle, which is the minimum number of iteration at which the optimal path length is obtained. The effect of frequency on the performance of the algorithm was also performed. In all, the Regular Falsi algorithm maintained the same convergence cycle

REFERENCES

1. Bi, S., Ho, C. K., & Zhang, R. (2015). Wireless powered communication: Opportunities and challenges. *IEEE Communications Magazine*, 53(4), 117-125.
2. Jedermann, R., Pötsch, T., & Lloyd, C. (2014). Communication techniques and challenges for wireless food quality monitoring. *Phil. Trans. R. Soc. A*, 372(2017), 20130304.
3. Ozuomba, Simeon, Constant Kalu, and Henry Johnson Enyenihi. "Comparative Analysis of the Circle Fitting Empirical Method and the International Telecommunication Union Parabola Fitting Method for Determination of the Radius of Curvature for Rounded Edge Diffraction Obstruction." *Communications* 7: 16-21.
4. Ozuomba, Simeon, Henry Johnson Enyenihi, and Constance Kalu. "Program to Determine the Terrain Roughness Index using Path Profile Data Sampled at Different Moving Window Sizes." *International Journal of Computer Applications* 975: 8887.
5. Eunice, Akinloye Bolanle, Simeon Ozuomba, and Isaac A. Ezenugu. "Evaluation of the Distribution of Terrain Roughness Index for Terrestrial Line of Site Microwave Links in Uyo Metropolis." *Mathematical and Software Engineering* 2.1 (2016): 9-18.
6. Kukshya, V. (2001). *Wideband Terrestrial Path Loss Measurement Results For Characterization of Pico-cell Radio Links at 38 GHz and 60 GHz Bands of Frequencies* (Doctoral dissertation, Virginia Tech).
7. Tse, D., & Viswanath, P. (2005). *Fundamentals of wireless communication*. Cambridge university press.
8. Asiyo, M. O., & Afullo, T. J. O. (2013). Statistical estimation of fade depth and outage probability due to multipath propagation in Southern Africa. *Progress In Electromagnetics Research*, 46, 251-274.
9. Kalu, Constance, Simeon Ozuomba, and Orogun Avuwakoghene Jonathan. "Rain Rate Trend-Line Estimation Models and Web Application For The Global Itu Rain Zones." *European Journal of Engineering and Technology* Vol 3.9 (2015).
10. Islam, R. U., Rahman, T. A., Rahim, S. K. B. A., Al-tabatabaie, K. F., & Abdulrahman, A. Y. (2009). Fade margins prediction for broadband fixed wireless access (BFWA) from measurements in tropics. *Progress In Electromagnetics Research*, 11, 199-212.
11. Cardoso, F. D., & Correia, L. M. (2002, September). Fading depth evaluation in mobile communications-from GSM to future mobile broadband systems. In *Personal, Indoor and Mobile Radio Communications, 2002. The 13th IEEE International Symposium on* (Vol. 1, pp. 125-129). IEEE.
12. Emenyi M., Udofia K. M. & Amaefule O. C., (2017). Computation of Optimal Path Length for Terrestrial Line of Sight Microwave Link Using Newton–Raphson Algorithm. *Software Engineering* Volume 5, Issue 3, May 2017, Pages: 44-50
13. Mohammad, H. (2015). A Simple Hybrid Method for Finding the Root of Nonlinear Equations.
14. McDougall, T. J., & Wotherspoon, S. J. (2014). A simple modification of Newton's method to achieve convergence of order. *Applied Mathematics Letters*, 29, 20-25.
15. Kou, J. (2007). The improvements of modified Newton's method. *Applied Mathematics and Computation*, 189(1), 602-609.
16. Intep, S. (2018). A Review of Bracketing Methods for Finding Zeros of Nonlinear Functions. *Applied Mathematical Sciences*, 12(3), 137-146.
17. Akram, S., & ul Ann, Q. (2015). Newton Raphson method. *International Journal of Scientific & Engineering Research*, 6(7).
18. Braun, T. R., & Smith, R. C. (2008). High speed model implementation and inversion techniques for ferroelectric and ferromagnetic transducers. *Journal of Intelligent Material Systems and Structures*, 19(11), 1295-1310.
19. Gottlieb, G. R., & Thompson, B. F. (2010). Bisectioned direct quadratic regulafalsi. *Appl. Math. Sci*, 4(15), 709-718.
20. Johnson, Enyenihi Henry, Simeon Ozuomba, and Ifio Okon Asuquo. "Determination of Wireless Communication Links Optimal Transmission Range Using Improved Bisection Algorithm." (2019).
21. Ehiwario, J. C., & Aghamie, S. O. (2014). Comparative Study of Bisection, Newton-Raphson and Secant Methods of Root-Finding Problems. *IOSR Journal of Engineering (IOSRJEN)*, 4(04).
22. Tanakan, S. (2013). A new algorithm of modified bisection method for nonlinear equation. *Applied Mathematical Sciences*, 7(123), 6107-6114.
23. Suhadolnik, A. (2012). Combined bracketing methods for solving nonlinear equations. *Applied Mathematics Letters*, 25(11), 1755-1760.
24. Srivastava, R. B., & Srivastava, S. (2011). Comparison of Numerical Rate of Convergence of Bisection, Newton-Raphson's and Secant Methods. *Journal of Chemical, Biological and Physical Sciences (JCBPS)*, 2(1), 472.
25. Iwetan, C. N., Fuwape, I. A., Olajide, M. S., & Adenodi, R. A. (2012). Comparative Study of the Bisection and Newton Methods in solving for Zero and Extremes of a Single-Variable Function. *J. of NAMP*, 21, 176.
26. Wu, H., Zhang, L., & Miao, Y. (2017). The propagation characteristics of radio frequency signals for wireless sensor networks in large-scale farmland. *Wireless Personal Communications*, 95(4), 3653-3670.
27. Sun, S., Thomas, T. A., Rappaport, T. S., Nguyen, H., Kovacs, I. Z., & Rodriguez, I. (2015, December). Path loss, shadow fading, and line-of-sight probability models for 5G urban macro-cellular scenarios. In *Globecom Workshops (GC Wkshps), 2015 IEEE* (pp. 1-7). IEEE.
28. Welch, B. W., & Piasecki, M. T. (2015). Earth-Facing Antenna Characterization in Complex Ground Plane/Multipath Rich Environment.

29. TSAI, M. (2011). Path-loss and shadowing (large-scale fading). *National Taiwan University October, 20, 2011*.
30. Schneider, T., Wiatrek, A., Preußler, S., Grigat, M., & Braun, R. P. (2012). Link budget analysis for terahertz fixed wireless links. *IEEE Transactions on Terahertz Science and Technology, 2(2)*, 250-256.
31. Rahimian, A., & Mehran, F. (2011, November). RF link budget analysis in urban propagation microcell environment for mobile radio communication systems link planning. In *Wireless Communications and Signal Processing (WCSP), 2011 International Conference on* (pp. 1-5). IEEE.
32. Rao, R. S. (2015). *Microwave engineering*. PHI Learning Pvt.Ltd.
33. Islam, R. U., Rahman, T. A., Rahim, S. K. B. A., Al-tabatabaie, K. F., & Abdulrahman, A. Y. (2009). Fade margins prediction for broadband fixed wireless access (BFWA) from measurements in tropics. *Progress In Electromagnetics Research, 11*, 199-212.
34. Ononiwu, G., Ozuomba, S., & Kalu, C. (2015). DETERMINATION OF THE DOMINANT FADING AND THE EFFECTIVE FADING FOR THE RAIN ZONES IN THE ITU-R P. 838-3 RECOMMENDATION. *European Journal of Mathematics and Computer Science Vol, 2(2)*.
35. Uslu, S., & Tekin, L. (2003). Path loss due to rain fading and precipitation in 26 GHz LMDS systems: consideration of implementation in Turkey. *Microwave and Telecommunication Technology, 68-72*.
36. Ozuomba, S., Kalu, C., & Obot, A. B. (2016). Comparative Analysis of the ITU Multipath Fade Depth Models for Microwave Link Design in the C, Ku, and Ka-Bands. *Mathematical and Software Engineering, 2(1)*, 1-8.
37. Gökteş, P. (2015). *Analysis and implementation of prediction models for the design of fixed terrestrial point-to-point systems* (Doctoral dissertation, bilkent university).
38. Meng, Y. S., & Lee, Y. H. (2010). Investigations of foliage effect on modern wireless communication systems: A review. *Progress In Electromagnetics Research, 105*, 313-332.
- Mohajer, M., Khosravi, R., & Khabiri, M. (2006, May). Flat Fading Modeling in Fixed Microwave Radio Links Based on ITU-R P. 530-11. In *Microwaves, Radar & Wireless Communications, 2006. MIKON 2006. International Conference on* (pp. 423-426). IEEE.